Lineshape of the thermopower of quantum dots

Fahlvik Svensson, Sofia; Persson, Ann; Hoffmann, E. A.; Nakpathomkun, N.; Nilsson, Henrik; Xu, Hongqi; Samuelson, Lars; Linke, Heiner

Published in:
New Journal of Physics

DOI:
10.1088/1367-2630/14/3/033041

2012

Lineshape of the thermopower of quantum dots

2012 New J. Phys. 14 033041

(http://iopscience.iop.org/1367-2630/14/3/033041)

New Journal of Physics
The open-access journal for physics

Lineshape of the thermopower of quantum dots

S Fahlvik Svensson[1,6], A I Persson[1,2], E A Hoffmann[2,3], N Nakpathomkun[2,4], H A Nilsson[1], H Q Xu[1,5], L Samuelson[1] and H Linke[1,2,6]

[1] Solid State Physics and the Nanometer Structure Consortium (nmC@LU), Lund University, PO Box 118, 221 00 Lund, Sweden
[2] Physics Department and Materials Science Institute, University of Oregon, Eugene, OR 97403, USA
[3] Center for NanoScience and Fakultät für Physik, Ludwig-Maximilians-Universität, Munich 80539, Germany
[4] Department of Physics, Thammasat University, Pathum Thani 12120, Thailand
[5] Key Laboratory for the Physics and Chemistry of Nanodevices and Department of Electronics, Peking University, Beijing 100871, People's Republic of China
E-mail: sofia.fahlvik_svensson@ftf.lth.se and heiner.linke@ftf.lth.se

New Journal of Physics **14** (2012) 033041 (11pp)
Received 11 October 2011
Published 28 March 2012
Online at http://www.njp.org/
doi:10.1088/1367-2630/14/3/033041

Abstract. Quantum dots are an important model system for thermoelectric phenomena, and may be used to enhance the thermal-to-electric energy conversion efficiency in functional materials, by tuning the Fermi energy relative to the dots' transmission resonances. It is therefore important to obtain a detailed understanding of a quantum dot's thermopower as a function of the Fermi energy. However, so far it has proven difficult to take the effects of interactions into account in the interpretation of experimental data. In this paper, we present detailed measurements of the thermopower of quantum dots defined in heterostructure nanowires. We show that the thermopower lineshape is described well by a Landauer-type transport model that uses as its input experimental values of the dot conductance, which contains information about interaction effects.

[6] Authors to whom any correspondence should be addressed.

Contents

1. Introduction

The thermovoltage, V_{th}, of a quantum dot (QD) is defined as the open-circuit voltage in response to an applied temperature differential, ΔT, and has already been explored [1, 2] as one of the fundamental electron transport characteristics of QDs. In recent years, the thermoelectric properties of QDs have attracted renewed interest because QDs are essentially highly tunable energy filters, which can be used to optimize their performance as thermoelectric power generators [3] or coolers [3, 4]. Specifically, QDs with a very narrow (delta-like) transmission resonance have been shown to be ideal thermoelectric energy converters: they can be operated reversibly, near the fundamental Carnot limit of their efficiency [3, 5, 6], and their efficiency at maximum power approaches the fundamental Curzon–Ahlborn limit [7–9]. The use of QDs (nanocrystals) embedded into bulk material [10] or nanowires [6] has been proposed as a way to enhance a material's thermopower or Seebeck coefficient, $S = V_{\mathrm{th}}/\Delta T$. Because the thermopower of ideal QDs depends only on fundamental constants, QDs have also been proposed as a quantum measurement standard for the Seebeck coefficient [11].

For each of these applications, as well as for fundamental understanding, it is important to know how V_{th} depends on the properties of the QD, as well as on the chemical potential in the electron reservoirs. For a dot with infinitely sharp, delta-like transmission resonances separated by an energy ΔE (figure 1), Beenakker and Staring [1] predicted a sawtooth-like dependence of V_{th} on the chemical potential, with a resulting maximum thermovoltage $V_{\mathrm{th}}^{\mathrm{max}} = (\Delta E/4e) \cdot (\Delta T/T)$. This model suggests that V_{th} of a QD can, in principle, be made arbitrarily large by decreasing the dot size, and thus increasing ΔE through charging or quantum confinement effects. Staring *et al* [2] did indeed find that the thermovoltage of a QD oscillates with a sawtooth-like lineshape for thermal energies kT much less than the QD's charging energy, e^2/C, but found a much lower amplitude than predicted. This difference was suggested to be due to the finite energy-broadening, Γ, of the levels in the QD (figure 1), a result of co-tunneling in the transport through the dot, which depends on the strength of the coupling to the leads [12]. Dzurak *et al* [13] shared this interpretation in the context of a similar experiment. Turek and Matveev [14] developed a thermopower theory including co-tunneling and predicted a transition, as a function of decreasing temperature, from a sawtooth-like lineshape to a lineshape more similar to an energy derivative of the dot's conductance. Kubala and König [15] later extended the theory to include all second-order tunneling contributions. Scheibner *et al* [16] observed the predicted transition, but it proved difficult to find detailed agreement between experiment and theory.

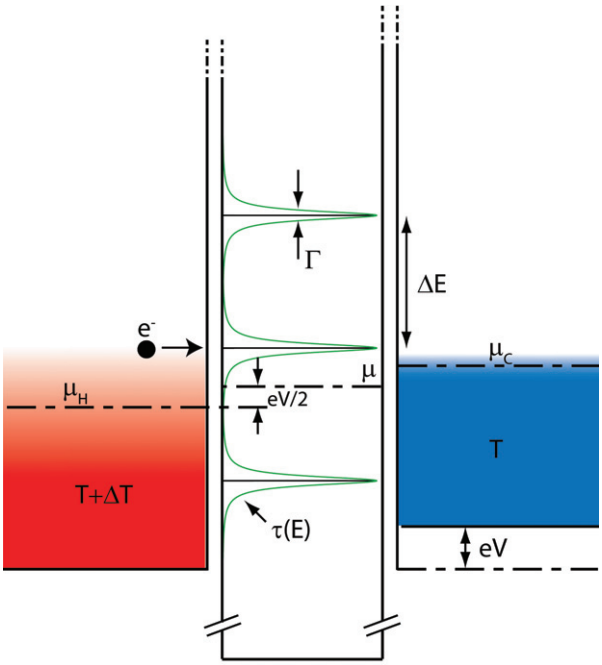

Figure 1. We consider a QD defined by a pair of energy barriers, and attached to a hot (left) and a cold (right) electron reservoir. The QD is characterized by an electron transmission function $\tau(E)$ consisting of Lorentzian resonances with full-width at half-maximum Γ and energy separation ΔE.

From these prior results it thus emerges that the lineshape of $V_{\rm th}$ of a QD depends on the energy scales kT and ΔE as well as on Γ. However, it is known that information about each of these parameters is contained in measurements of the conductance, G, of a QD. Here, we present detailed measurements of $V_{\rm th}$ and G in two different QDs defined in heterostructure nanowires. We show that, using measurements of G as a function of the chemical potential in the electron reservoirs as an input, and using a simple tunneling model implemented by a Landauer-type formalism, we can predict $V_{\rm th}$ as a function of the chemical potential for various $\Delta E/kT$ and Γ/kT. This approach takes into account transport through all-order tunneling processes by using an experimentally determined Lorentzian transmission function with finite broadening Γ. We begin by presenting our experimental results and will then turn to a comparison with the model.

2. Experiment

We used two QDs with different Γ and ΔE, each defined by an InP double-barrier structure embedded in an InAs nanowire, grown using metal–particle seeded growth and chemical beam epitaxy [17, 18]. For sample 1, denoted as QD1, $InAs_{0.8}P_{0.2}$ was used as the dot material (reducing the effective InP barrier height), and for sample 2, denoted as QD2, InAs was the dot material. Scanning electron microscope (SEM) inspection after the measurements showed that for QD1 (QD2) the nanowire diameter was 66 nm (55 nm) and the length of the QD (along the wire) was about 190 nm (10 nm).

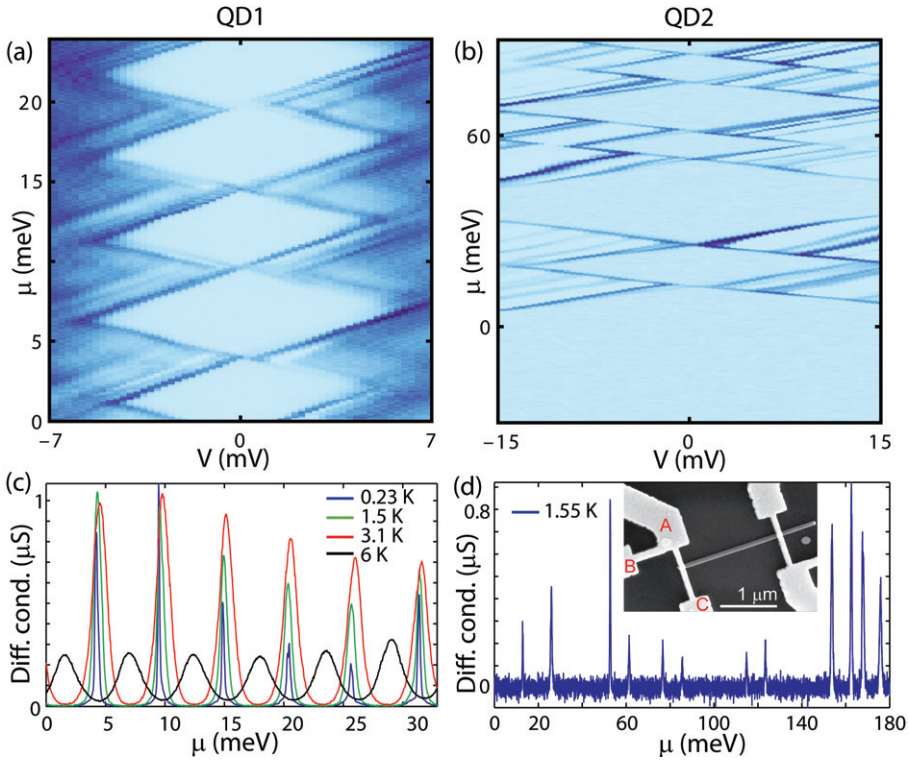

Figure 2. Differential conductance as a function of source–drain bias, V, and gate voltage, V_g, for (a) QD1 at a temperature $T = 0.23\,K$ and (b) QD2 at a temperature $T = 1.55\,K$, with the vertical axis already converted to μ (arbitrary zero). Differential conductance peaks measured as a function of μ at $V = 0$ for (c) QD1 and (d) QD2 are used to extract values for ΔE and Γ. The shift of energy levels at $T = 6\,K$ for QD1 is related to a gate shift. The inset of (d) shows an SEM image of the contact configuration used for both devices.

After growth, the nanowire was transferred to an n-doped Si wafer with a 100 nm thick SiO_X capping layer. The SiO_X/Si substrate acts as a global gate for tuning the QD states relative to the chemical potential in the leads. Ohmic Au/Ni contacts were fabricated by electron beam lithography, followed by passivation, metallization and lift-off [19, 20]. A three-terminal configuration is used to contact each of the two ends of the nanowire (see the inset of figure 2(d)). An ac heating current, I_H, applied through terminals A and C, is used to warm the contact electron gas [21]. I_H is applied in a push–pull fashion using a home-built, tunable operational-amplifier circuit such that I_H does not influence the voltage at the nanowire. Terminal B is used to assist in the tuning process. The drain contact temperature at the opposite end of the nanowire increases via electron–phonon coupling in the nanowire [21]. For QD2 we measure ΔT using QD thermometry [21]. For QD1 we use finite element modeling [21], which delivers results consistent with those from QD thermometry, to estimate the effective temperature differential ΔT applied across the wire at a given cryostat temperature and I_H.[7]

[7] The actual electronic temperature differential across the QD is expected to be about a factor 2–3 smaller than ΔT due to a temperature drop in the InAs leads [21].

The heating current, at frequency f, generates a thermovoltage, $V_{\rm th}$, composed of two distinguishable signals: (i) an ac thermovoltage at frequency $2f$ (because $V_{\rm th} \propto \Delta T \propto I_{\rm H}^2$), and (ii), after time-averaging, a dc thermovoltage. For QD1, the ac thermovoltage was measured using a standard lock-in technique to detect the second harmonic signal at frequency $2f$ (here $f = 13\,{\rm Hz}$). The lock-in measurements have the advantage of being relatively fast ($\leqslant 1\,{\rm s}$ per data point) without sacrificing the signal-to-noise ratio. For QD2, the dc component of $V_{\rm th}$ was measured. Any background signal (voltage measured when $I_{\rm H} = 0$) is subtracted from subsequent raw voltage data measured when $I_{\rm H} \neq 0$. Additional details are available elsewhere [22]. To isolate the dc signal, a low-pass resistor–capacitor (RC) filter damps ac components and therefore measurements on QD2 require slow sampling rates (several seconds per data point, using a multimeter with 1 s integration time).

Data that provide a basic characterization of QD1 and QD2 are shown in figure 2. From measurements of the differential conductance, $G = {\rm d}I/{\rm d}V$, as a function of gate voltage $V_{\rm g}$ (see figures 2(a) and (b)), we convert $V_{\rm g}$ to an energy scale, μ [23]. In figures 2(c) and (d), we plot G at $V = 0$ as a function of μ for both the samples. For QD1, the larger of the two dots, conductance peaks are spaced equally, indicating that the observed $\Delta E \approx 5.3\,{\rm meV}$ is the charging energy $E_{\rm C} = e^2/C$. To determine Γ for QD1, we fit the measured G to the derivative of the Landauer equation (see equation (1) below) at the lowest measured temperature, with the amplitude, A, and width, Γ, of the transmission function (equation (2)) used as free parameters. Averaged over multiple peaks we find that $\Gamma \approx 160\,\mu{\rm eV}$, corresponding to 1.8 K. The smaller QD2 has unequally spaced resonances due to quantum confinement effects, with $E_{\rm C} = 8.7\,{\rm meV}$. Because of a limitation in the temperature range of the cryostat, fitting G of QD2 produces only an approximate upper limit of $\Gamma \approx 30\,\mu{\rm eV}$, almost an order of magnitude less than in QD1.

In figure 3, we plot the thermovoltage of QD1 as a function of μ for different I_H and cryostat temperature T, allowing us to vary the relative energy scales Γ/kT and $\Delta E/kT$. At the highest temperature of 6 K an offset, presumably due to the thermovoltage in the InAs leads[8], has been added to center the thermovoltage curves at $V_{\rm th} = 0$.

The following observations can be made from figure 3: (i) $V_{\rm th}$ increases with $I_{\rm H}$ as expected in the linear response regime; (ii) at the lowest cryostat temperature ($T = 232\,{\rm mK}$), the lineshape of $V_{\rm th}$ resembles an energy derivative of G; and (iii) with increasing T, resulting in a decrease of Γ/kT and $\Delta E/kT$, $V_{\rm th}$ becomes more triangular. We will return to these observations after introducing our model.

3. Model

We use a Landauer-type approach in which the current through a QD connected to a cold (C) and a hot (H) reservoir is given by

$$I = \frac{2e}{h} \int [f_C\,(E, \mu_C, T) - f_H\,(E, \mu_H, T{+}\Delta T)]\tau(E){\rm d}E, \tag{1}$$

where $f_{\rm C/H}$ is the Fermi–Dirac distribution on the hot (H) and cold (C) sides, respectively, $\mu_{C/H}$ are the chemical potentials in the reservoirs, T and $T + \Delta T$ are the electronic temperatures, and $\tau(E)$ is the transmission function of the QD (figure 1). Usually, equation (1) is used to describe

[8] The offset, as shown in the inset to figure 3, increases with heating current. We estimate ΔT to be about 30–50 mK using a heating current of 85 mA, which results in $S \approx 40\,\mu{\rm V\,K^{-1}}$, which is comparable to the value of $120\,\mu{\rm V\,K^{-1}}$ measured for similar InAs nanowires at the higher temperature of 100 K [24].

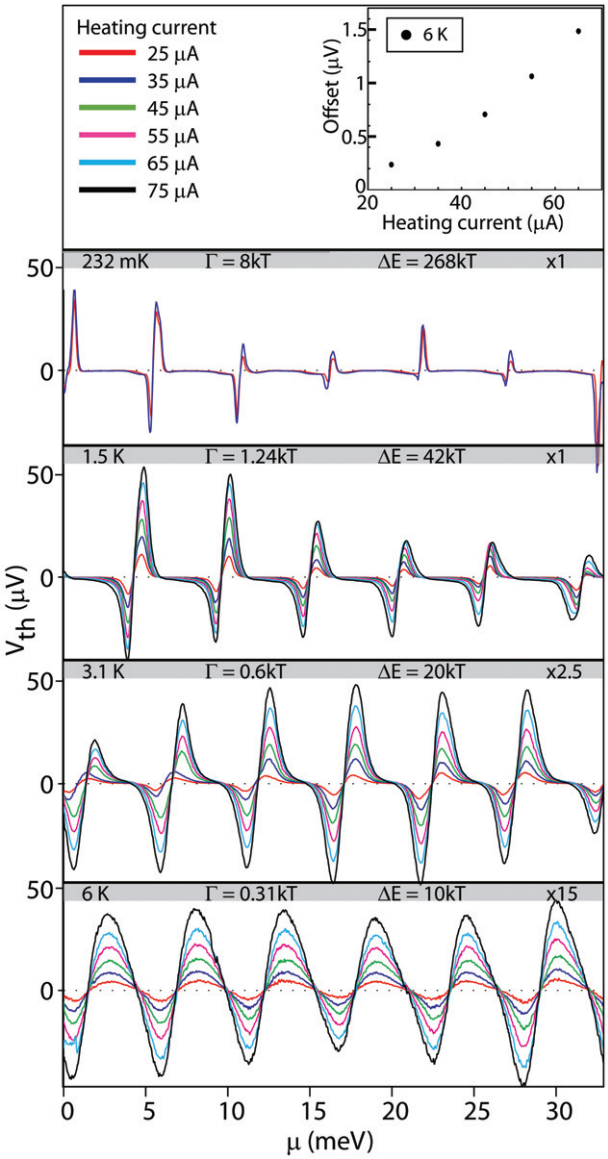

Figure 3. Thermovoltage of QD1 as a function of μ (arbitrary zero) for different T and heating currents I_{H}. Note that the same I_{H} applied at higher T causes a smaller ΔT. At the highest temperature of 6 K an offset (inset) has been subtracted to center the thermovoltage curves at $V_{\mathrm{th}} = 0$ V (see text). The thermovoltage signals at $T = 3.1$ K and 6 K were scaled as indicated.

elastic, non-interacting transport processes. Note, however, that $\tau(E)$ can be used to take into account additional effects [25]. We approximate $\tau(E)$ as the sum of Lorentzian functions,

$$\tau\,(E) = \sum_n A_n \frac{(\Gamma_n/2)^2}{(E-E_n)^2 + (\Gamma_n/2)^2}, \tag{2}$$

with their centers located at the dot's resonant levels E_n, with widths Γ_n and amplitudes A_n. For computational reasons it is convenient to define the average chemical potential $\mu = (\mu_{\mathrm{C}} + \mu_{\mathrm{H}})/2$

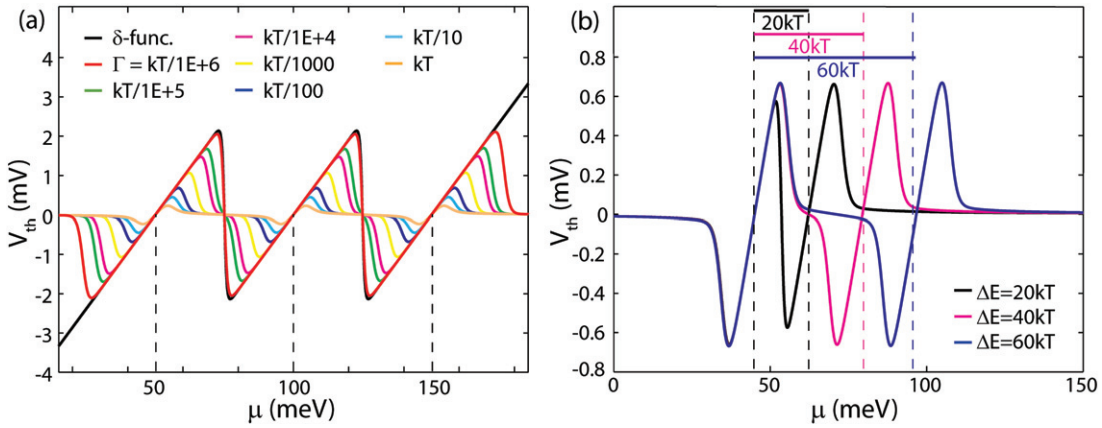

Figure 4. Modeling data based on equation (3) for $T = 10\,\mathrm{K}$ and $\Delta T = 1\,\mathrm{K}$. (a) $V_{\mathrm{th}}(\mu)$ for varying Γ and for $\Delta E = 50\,\mathrm{meV} \approx 58\,kT$. The dashed lines indicate positions E_n of resonance levels. (b) $V_{\mathrm{th}}(\mu)$ for $\Gamma = kT/100$ and for varying ΔE. The blue graphs in (a) and (b) correspond to approximately equivalent conditions, $\Gamma = kT/100$ and $\Delta E \approx 60\,kT$. The μ-axes use an arbitrary zero.

and to assume that V is applied symmetrically across the dot such that $\mu_{\mathrm{C/H}} = \mu \pm \mathrm{eV}/2$. We calculate $S = V_{\mathrm{th}}/\Delta T$ using the approximation [11, 26]

$$S = \frac{V_{\mathrm{th}}}{\Delta T} = -\frac{1}{e\,(T+\Delta T/2)} \frac{\int (E-\mu)\,\frac{\partial f_0}{\partial E}\,\tau\,(E)\,\mathrm{d}E}{\int \frac{\partial f_0}{\partial E}\,\tau\,(E)\,\mathrm{d}E}. \tag{3}$$

Here, f_0 is the equilibrium Fermi–Dirac distribution for $\Delta T = 0$ and $V = 0$, and $\mathrm{eV_{th}} \ll \Delta E$ and $\Delta T \ll T$ was assumed in the derivation of equation (3).[9]

Figure 4(a) plots V_{th} as a function of μ for a QD with resonant energy levels of width Γ varying over a wide range, from $10^{-6}kT$ to kT and for $\Delta E/kT \gg 1$. Also plotted in figure 4(a), for comparison, is the ideal sawtooth lineshape predicted by Beenakker and Staring [1] and obtained from equation (3) when $\tau(E)$ consists of delta functions ($\Gamma \to 0$). A key observation in figure 4(a) is that the lineshape of $V_{\mathrm{th}}(\mu)$ deviates from the sawtooth lineshape for Γ as small as $10^{-5}kT$, i.e. even for exceedingly small coupling to the leads. With increasing Γ, the lineshape increasingly resembles the shape of an energy derivative of the conductance peaks, V_{th} between transmission resonances becomes suppressed and the amplitude of the V_{th} resonances is, for finite Γ, much lower than predicted in [1].

The single-electron tunneling picture combined with the Landauer equation (equation (1)) provides a conceptual explanation for the observations in figure 4(a). First, we recall that V_{th}, for a given configuration (ΔT, μ), can be found by looking for the value of the bias voltage where $I = 0$ (open-circuit condition). When $\tau(E)$ is a delta function, zero current across the dot is obtained when $\tau(E)$ is at the position where the term $\Delta f = f_{\mathrm{C}} - f_{\mathrm{H}} = 0$ (this is the

[9] As is common in thermoelectrics, we use the approximate equation (3) for numerical convenience. A different, more time-consuming method is to use equation (1) to calculate the current I for all external bias voltages, V, and to search for the V at which $I = 0$ for each μ. We confirmed for representative parameters that the results from both approaches agree within the resolution of our figures. Note that equation (3) is identical to equation (5) in [11] where T was defined as the average temperature of the reservoirs.

condition of energy-specific equilibrium as defined in [27]). This condition yields the sawtooth lineshape [1]. For finite Γ, when $\tau(E)$ is slightly broadened, charge carriers can leak through the tails of the Lorentzian. Because Δf is not antisymmetric for finite bias voltage, a correction in bias voltage is needed at a given $|\mu - E_n|$ in order to cancel the leakage current and thereby maintain the zero-current condition. As a result the slope of $V_{\rm th}(\mu)$ is slightly reduced for small $|\mu - E_n|$ (not visible in figure 4(a)) [11], and drops for larger $|\mu - E_n|$. However, Δf goes to zero faster as a function of energy than a Lorentzian, such that the Lorentzian's tails will always sample all of Δf. Therefore, for larger Γ and larger $|\mu - E_n|$, the zero-current condition can only be maintained with $V_{\rm th}$ going to zero.

In figure 4(b), we plot $V_{\rm th}$ as a function of ΔE for fixed $\Gamma = 0.01\,kT$. As ΔE decreases, $V_{\rm th}$ becomes more triangular, its negative slope between resonances becomes steeper and its amplitude decreases. It is worth noting that, with a decrease in ΔE, this effect becomes significant already when $\Delta E \sim 10\,kT$ and $\Delta E \sim 10^3\Gamma$.

4. Discussion

Qualitatively, our experimental data (figure 3) at the lowest temperature show a derivative-like lineshape, in agreement with our model in figure 4(a). When T is increased in the experiment, $V_{\rm th}$ becomes more triangular (figure 3), consistent with our modeled data in figure 4(b), suggesting that the leading cause of the experimentally observed lineshape evolution is the decrease of $\Delta E/kT$ with increasing T.

We now turn to a more quantitative comparison of the experiment and the model. In figure 5(a), we show S of QD1 at four different temperatures with $I_{\rm H}$ chosen such that we estimate (based on finite-element modeling [21]) a ΔT of a few 10 mK for each data set. In figure 5(b), we show the corresponding modeling results based on equation (3), which used as their only input T and ΔT, as well as $\Gamma = 160\,\mu$eV and $\Delta E = 5.3$ meV as determined experimentally (see figure 2(c)). There is good agreement between experiment and theory at the two lowest temperatures, while the suppression of S between transmission resonances is stronger in the experiment at higher T. $V_{\rm th}$ of QD1 was measured using an ac technique, and therefore the observed suppression might be due to RC damping as the dot's resistance (and therefore the system's RC constant) increases between the resonances. Therefore, in figure 5(c), we include the effect of RC damping (at frequency $f = 13$ Hz) using $R(\mu)C = C/G(\mu)$ based on measured data for $G(\mu)$ and the modeled data from figure 5(b). For the capacitance to ground, C, we estimate an upper limit of 0.5 nF, with the leading contribution from the cryostat leads (≈ 0.4 nF) estimated to be much larger than those from the bond pads and the QD itself. After taking the RC damping into account, the agreement of the model with the experiment is excellent (see figures 5(a) and (c)), given the uncertainty in the accuracy of the modeled ΔT.

A similar comparison between experiment and model is shown in figures 5(d)–(f) for QD2, measured using the dc technique, and for smaller values of Γ/kT and larger values of $\Delta E/kT$ than in figures 5(a)–(c). Also, here experiment (figure 5(d)) and theory (figure 5(e)) are in very good agreement for the lowest temperature. At higher temperatures, the model predicts increasing amplitudes of S due to the decrease in Γ/kT. However, the same increase is not seen in experiment, where instead S appears to be suppressed compared to the model. To improve the agreement between theory and experiment, we include the effect of the finite load resistance, $R_{\rm L} = 47\text{M}\Omega$, of the dc measurement setup, which is expected to reduce the measured

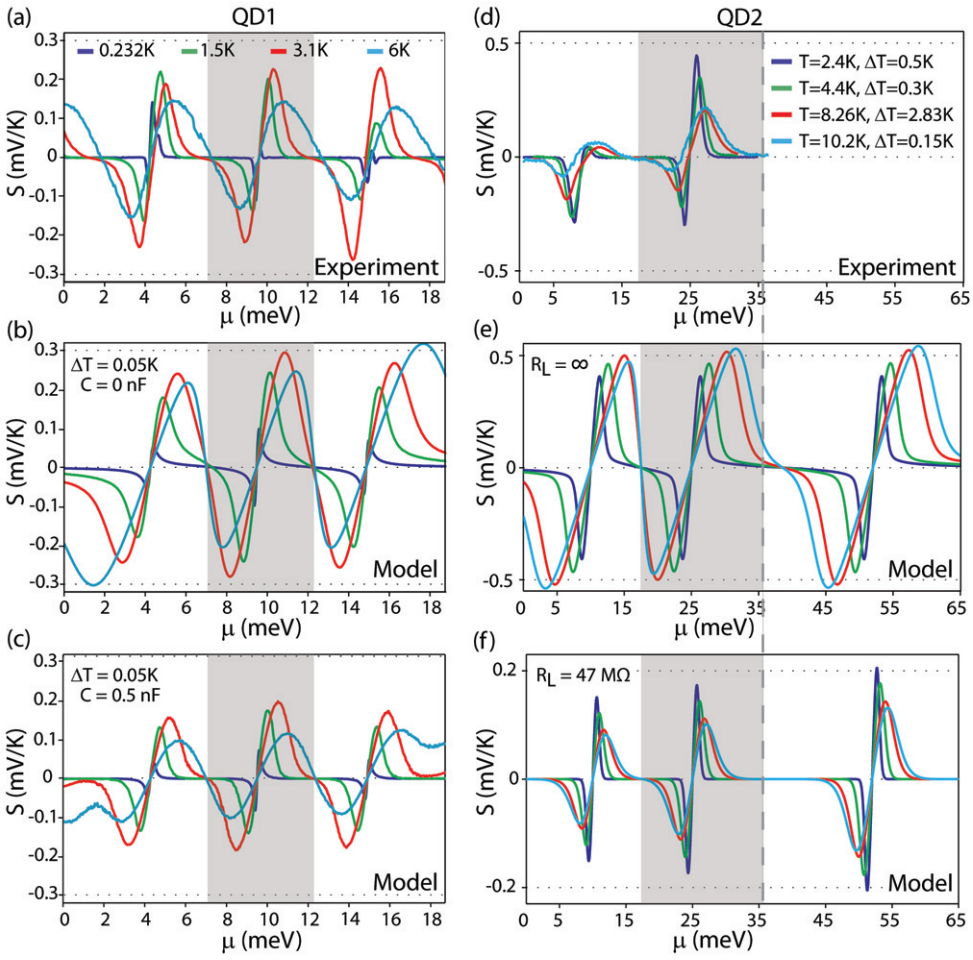

Figure 5. (a) Thermopower, $S = V_{\rm th}/\Delta T$, for QD1 at the indicated cryostat temperatures, based on the values for ΔT obtained using finite-element simulations [21]: $\Delta T \approx 0.035\,{\rm K}$ at $T = 0.232\,{\rm K}$, $\Delta T \approx 0.05\,{\rm K}$ at $T = 1.5\,{\rm K}$, $\Delta T \approx 0.045\,{\rm K}$ at $T = 3.1\,{\rm K}$ and $\Delta T \approx 0.01\,{\rm K}$ at $T = 6\,{\rm K}$. (b) Modeling results based on equation (3) for the same T as in (a), $\Delta T = 0.05\,{\rm K}$, $\Delta E = 5.3\,{\rm meV}$ and $\Gamma = 160\,\mu{\rm eV}$. (c) The same data as in (b), but including the effect of RC damping in the measurement circuit, using the measured $R = 1/G$ and a fixed $C = 0.5\,{\rm nF}$. Note that the model used only three resonances and therefore only the center resonance (highlighted by gray background) experiences the effect of neighboring resonances present in the experiment and corresponds to the data in (a). (d) Thermopower, S, of QD2 at cryostat temperatures T and ΔT as indicated. Here ΔT was measured using QD thermometry [21]. Γ/kT varies here from 0.145 at 2.4 K to 0.042 at 8.26 K, and $\Delta E/kT$ from 73 at 2.4 K to 21 at 8.26 K. (e) Modeled data based on equation (3) for the same T, ΔT, ΔE and Γ_n as in (d). Note that the model took into account a third resonance that was present in the device. Only the center resonance in (e) can be compared to (d). (f) The same data as in (e), including the effect of the finite load resistance, $R_{\rm L}$, of the experimental setup.

thermovoltage compared to the dot's actual thermovoltage by a factor of $(1 + R(\mu, T)/R_L)^{-1}$ (for details, see [22]). Because we do not have data on the dot's resistance, $R(\mu, T) = 1/G(\mu, T)$, at all temperatures, we model $G(\mu, T)$ using the equation

$$G(\mu, T) = \frac{1}{kT} G_0 \operatorname{sech}^2\left(\frac{\mu - E_n}{2kT}\right), \tag{4}$$

which is obtained from the derivative of the Landauer equation with respect to bias voltage for $\Gamma \ll kT$ [28], where G_0 is a fit parameter that we obtain by matching the measured $G(\mu)$ at $T = 1.55\ K$ (figure 2(d)), and E_n is the position of the nth resonance as defined in equation (2). In figure 5(f), we show the effect of this expected suppression on the modeled thermopower data of figure 5(e), and find that the qualitative agreement with the experiment in figure 5(d) is now excellent. The remaining quantitative discrepancy, roughly a factor of 2, might be related to an inaccuracy in the value of Γ used in the thermopower model in figure 5(e). To obtain a more accurate value for Γ, conductance measurements at lower temperatures $T \approx \Gamma/k$ would be required. Note that the experimental data also show a curious asymmetric lineshape (of the leftmost resonance), indicating that higher-order effects may be important [29].

5. Conclusion

In conclusion, we have tested the extent to which a simple Landauer-type model predicts the lineshape of the thermopower S in quantum dots as a function of the relevant energy scales Γ/kT and $\Delta E/kT$, which are readily available from conductance measurements. Using high-quality experimental data that allow for a detailed comparison with theory, we find excellent qualitative agreement and reasonable quantitative agreement, when the effects of the measurement setup are taken into account in the model.

In our approach, we used a Landauer-type equation (which is normally used for elastic, non-interacting processes) and took into account additional information, namely about the coupling of the dot states to the leads, and about interactions in the dot, by using a $\tau(E)$ based on experimental measurements. For an interacting system such as that considered here, this approach is strictly valid only in the linear response regime and at zero temperature [25]. The model can therefore be expected to break down at finite T or finite ΔT, because inelastic processes may become important in these cases. In our experiments, the temperature was small ($kT/\Delta E \ll 1$) and the system was, in this respect, in the linear-response regime, with ΔT an order of magnitude smaller than T. However, we cannot rule out spin-flip processes in our experiment, and it is not obvious why our assumption of non-interacting particles works so well.

Acknowledgments

This work was supported by the Swedish Energy Agency *Energimyndigheten* (grant no. 32920-1), the Office of Naval Research (grant no. N00014-05-1-0903), an NSF-IGERT Fellowship, the Royal Physiographic Society in Lund, the Sweden–America Foundation, the Thai Government, the Swedish Foundation for Strategic Research (SSF), the Swedish Research Council (VR), the Knut and Alice Wallenberg Foundation and the Nanometer Structure Consortium at Lund University (nmC@LU).

References

[1] Beenakker C W J and Staring A A M 1992 *Phys. Rev.* B **46** 9667
[2] Staring A A M, Molenkamp L W, Alphenaar B W, Vanhouten H, Buyk O J A, Mabesoone M A A, Beenakker C W J and Foxon C T 1993 *Europhys. Lett.* **22** 57
[3] Humphrey T E, Newbury R, Taylor R P and Linke H 2002 *Phys. Rev. Lett.* **89** 116801
[4] Edwards H L, Niu Q, Georgakis G A and Delozanne A L 1995 *Phys. Rev.* B **52** 5714
[5] Mahan G D and Sofo J O 1996 *Proc. Natl Acad. Sci. USA* **93** 7436
[6] O'Dwyer M F, Humphrey T E and Linke H 2006 *Nanotechnology* **17** S338
[7] Esposito M, Lindenberg K and Van den Broeck C 2009 *Europhys. Lett.* **85** 60010
[8] Esposito M, Kawai R, Lindenberg K and Van den Broeck C 2010 *Phys. Rev.* E **81** 041106
[9] Nakpathomkun N, Xu H Q and Linke H 2010 *Phys. Rev.* B **82** 235428
[10] Cai J W and Mahan G D 2008 *Phys. Rev.* B **78** 035115
[11] Mani P, Nakpathomkun N, Hoffmann E A and Linke H 2011 *Nano Lett.* **11** 4679
[12] König J, Schoeller H and Schön G 1997 *Phys. Rev. Lett.* **78** 4482
[13] Dzurak A S, Smith C G, Barnes C H W, Pepper M, MartinMoreno L, Liang C T, Ritchie D A and Jones G A C 1997 *Phys. Rev.* B **55** 10197
[14] Turek M and Matveev K A 2002 *Phys. Rev.* B **65** 115332
[15] Kubala B and König J 2006 *Phys. Rev.* B **73** 195316
[16] Scheibner R, Novik E G, Borzenko T, Konig M, Reuter D, Wieck A D, Buhmann H and Molenkamp L W 2007 *Phys. Rev.* B **75** 041301
[17] Persson A I, Fröberg L E, Jeppesen S, Björk M T and Samuelson L 2007 *J. Appl. Phys.* **101** 034313
[18] Fröberg L E, Wacaser B A, Wagner J B, Jeppesen S, Ohlsson B J, Deppert K and Samuelson L 2008 *Nano Lett.* **8** 3815
[19] Thelander C, Björk M T, Larsson M W, Hansen A E, Wallenberg L R and Samuelson L 2004 *Solid State Commun.* **131** 573
[20] Suyatin D B, Thelander C, Björk M T, Maximov I and Samuelson L 2007 *Nanotechnology* **18** 105307
[21] Hoffmann E A, Nilsson H A, Matthews J E, Nakpathomkun N, Persson A I, Samuelson L and Linke H 2009 *Nano Lett.* **9** 779
[22] Hoffmann E A, Nilsson H A, Samuelson L and Linke H 2011 *AIP Conf. Proc.* **1399** 397
[23] 1992 *Single Charge Tunneling (NATO ASI Series B294)* ed H Grabert and M H Devoret (New York: Plenum) p 176
[24] Zhou F 2009 Thermoelectric transport in semiconducting nanowires *PhD Thesis* University of Texas at Austin
[25] Meir Y and Wingreen N S 1992 *Phys. Rev. Lett.* **68** 2512
[26] Dubi Y and Di Ventra M 2011 *Rev. Mod. Phys.* **83** 131
[27] Humphrey T E and Linke H 2005 *Phys. Rev. Lett.* **94** 096601
[28] Hoffmann E A 2009 The thermoelectric efficiency of quantum dots in InAs/InP nanowires *PhD Thesis* University of Oregon
[29] Costi T A and Zlatic V 2010 *Phys. Rev.* B **81** 235127